ISIJ International, Vol. 38 (1998), No. 4, pp. 348–356

Development of Double and Single Hot Thermocouple Technique for *in Situ* Observation and Measurement of Mold Slag Crystallization

Yoshiaki KASHIWAYA, Carlos E. CICUTTI,[1] Alan W. CRAMB[2] and Kuniyoshi ISHII[3]

Formerly Faculty of Engineering, Hokkaido University. Now at Department of Materials Science and Engineering, Carnegie Mellon University, Pittsburgh, PA, USA. 1) Formerly Department of Materials Science and Engineering, Carnegie Mellon University. Now at Center for Industrial Research, FUDETEC, Argentina. 2) Department of Materials Science and Engineering, Carnegie Mellon University, 5000 Forbes Ave., Pittsburgh, PA 15213, USA.
3) Department of Materials Science and Engineering, Faculty of Engineering, Hokkaido University, Kita-ku, Sapporo, Hokkaido, 060-8628 Japan.

(Received on September 17, 1997; accepted in final form on December 16, 1997)

To overcome the limitations of differential thermal analysis (DTA) and direct casting experimentation in the measurement and understanding of the solidification phenomena of mold slags, the double and single hot thermocouple techniques (DHTT and SHTT) for the direct observation and measurement of mold slag crystallization were developed. These methods enable the solidification and melting process of transparent slags to be observed *"in situ"* under conditions where the temperature or temperature gradient can be measured and controlled. The SHTT allows a sample to be subjected to rapid cooling rates or to be held under isothermal conditions. The DHTT allows large temperature gradients to be developed between the two thermocouples and allows a simulation of the transient conditions which can occur in the infiltrated slag film that occurs between the mold and the solidifying shell in the mold of a continuous caster. By these techniques both isothermal and non-isothermal phenomena can be studied.

A number of mold slags are optically transparent or translucent at steelmaking temperatures while the crystalline phase which precipitates upon cooling is opaque and can be clearly observed using optical microscopy. Thus the SHTT and DHTT are connected to an image capturing and analysis system that allows the onset and growth of the opaque crystals which precipitate from the slags to be documented. The development and application of these techniques to mold slag crystallization will be discussed in this paper.

KEY WORDS: hot thermocouple; mold flux; continuous casting; crystallization; nucleation; crystal growth; silicate; slag; TTT; CCT.

1. Introduction

Mold slags* play an important role in the control of the continuous casting process and an understanding of mold slag properties and solidification behavior is the basis for optimization of continuous caster operation.[1–19] The precipitation of crystalline solids from mold slags during continuous casting is well documented and the use of casting powders with a high crystallization tendency*2 has been reported to be beneficial in the casting of peritectic steel grades where the formation of a significant crystal fraction in the mold slag layer between the mold and the strand reduces mold heat flux and helps alleviate problems with longitudinal cracking.[2–7] A high crystallization tendency has, however, been shown to be deleterious to caster operation under high speed casting conditions where increased friction between the mold and the strand and a higher incidence of sticking type breakouts has been documented.[8–15] For example, friction measurements carried out by Gilles *et al.*[15] in a slab caster showed that powders with a higher crystallization temperature gave larger friction forces while Hering *et al.*[9] noted that friction in the continuous casting mold depends on the viscosity of mold slag and the type of crystalline phases present.

The influence of crystalline phases on heat transfer in the mold has been the subject of a number of investigations.[2–6,16–18] In general, it is commonly accepted that a larger proportion of crystalline phases (or a casting powder with higher crystallization temperature) in a

* Mold slags are the liquids that form upon the melting of the mold powders or mold fluxes that are added to the mold of a continuous caster used in the processing of liquid steel. The mold slag composition can be slightly different in composition from the mold powder or flux due to absorption of inclusions or reaction with the liquid steel.

*2 Usually defined by the temperature at which crystallization can be measured during cooling using Differential Thermal Analysis (DTA).

liquid slag film decreases the overall heat transfer rate through the slag layer. This has been observed both in laboratory experiments[3] and in plant trials.[2,3] This reduction in the heat transfer has been attributed to the formation of pores in the crystalline layer[4] and to the scattering of radiation by the crystals, which reduces the radiative portion of the overall heat flux.[6] Jenkins[7] has modelled heat transfer across the slag film present between the shell and mold of a continuous caster and has shown that the relative position of the crystalline layer in the slag film can also modify the total rate of heat transfer that be found in the mold of a continuous caster. Thus it is necessary to understand the exact thermal conditions for precipitation and growth of a crystalline phase from a slag to understand the heat flux encountered in the mold of a continuous caster, while it is necessary to understand the crystal morphology and the temporal development of the fraction of solid to understand lubrication.

Quantification of mold slag solidification phenomena is normally conducted using differential thermal analysis (DTA) or slag casting in a chill mold; however, these techniques are limited as there is no direct method of observation of the solidification phenomena and only effects which liberate significant quantities of heat can be measured. The DTA is one of the most popular techniques for the study of slag crystallization. In this case, the slag sample is melted in a furnace and then cooled, together with a reference substance, and the temperature difference between both the sample and the reference material is recorded. When a reaction that involves heat generation or heat absorption takes place in the sample, a temperature difference between the sample and the reference can be detected. During sample cooling in a DTA, the highest temperature associated with an exothermic peak is usually called the "Crystallization Temperature" of the casting powder. In general, a higher "Crystallization Temperature" is thought to be related to a higher fraction of crystalline phase in the mold slag layer between the mold and the strand. However, a unique criteria to establish the cooling rate of the sample has not been established in these studies and only a few studies have considered the effect of the cooling rate on crystallization behavior.[16-18] Furthermore, the term "Crystallization Temperature" is sometimes confused with the so called "Solidification Temperature" of the slag which is determined from viscosity tests where a rapid rate of viscosity increase with decreasing temperature is incorrectly used as an indication of the onset of crystallization within the slag.[19]

Another technique that is frequently employed to determine the crystallization behavior of a mold slag consists of melting the mold slag sample and elevating its temperature to 1 550°C before quenching in a metallic mold.[9,11,12,16,18] After casting, the sample can be inspected at room temperature by different techniques. For example, the proportion of crystalline and glassy phases can be evaluated using microscopy and X-ray diffraction can be performed to determine the composition of the crystalline phases present. Obviously, these methods are useful to define a "crystallinity index" which compares, qualitatively, the tendency of different slags to give glassy or crystalline phases; however, these indexes do not provide a quantitative measurement that can characterize the slag behavior in the mold.

To properly characterize the precipitation of a second solid phase from a liquid, it is necessary to define the thermal field, the phase diagram and the nucleation and growth behavior of the solid. In mold slags, which are liquid oxides and easy glass formers under high cooling rates, it is necessary to be able to describe the conditions under which glass formation is possible, the conditions for the initiation of solidification, the crystal morphology, chemistry and growth rate and the time evolution of the fraction of solid. It is well known from classical nucleation theory that the onset of crystallization in slags must be a function of cooling rate and that to determine the solidification behavior of a liquid slag one must construct either isothermal time temperature transformation diagrams (TTT curves) or continuous cooling transformation diagrams (CCT curves). In addition, the growth rate, morphology and solidified fraction of the slag under varying cooling rates are important in the determination of the effect of crystallization of the slag on heat transfer and rheology. Thus a technique, whereby the thermal field can be determined as the solidification process is observed, was developed. This technique which combines the hot thermocouple technique with video observation and image analysis which allows crystal growth rates, morphologies and solidified fractions to be determined under defined thermal conditions.

The concept of the single hot thermocouple technique dates back to the end of nineteenth century and the hot thermocouple method itself was successfully developed by Ordway[20] and Welch, *et al.*[21] in 1950's. The progress of electronic development has made the hot thermocouple method easier and more reliable and has lead to renewed interest in the technique. Yanagase and Morinaga reported new developments of the hot thermocouple method and its application[22-24] in the 1970's and in 1980, Ohta *et al.*[24] applied the hot thermocouple method to the measurement of liquidus temperatures, clarification of the existence of two phase regions in slags and also to the understanding of slag reactions. More recently (1993) Asayama, *et al.*[25] has discussed glass formation in silicate slags using the hot thermocouple method.

Ishii and Kashiwaya first developed the double hot thermocouple method and applied it to a microgravity experiment to determine the microstructural change of a superconducting oxide in 1992.[27-29] The technique was also used by Murayama, *et al.*[26] to study Marangoni flow in silicate slags under microgravity and by Kuranaga *et al.*[27] to measure the ultimate length of a silicate slag film to clarify the mechanism of the separation of a bubble from a liquid slag surface.

In this paper, the application of the hot thermocouple method to the study of the crystallization of a mold slag will be described. Results of *in situ* observation and measurement of industrial and simulated mold slags will be shown using the single hot thermocouple technique (SHTT) and the double hot thermocouple technique

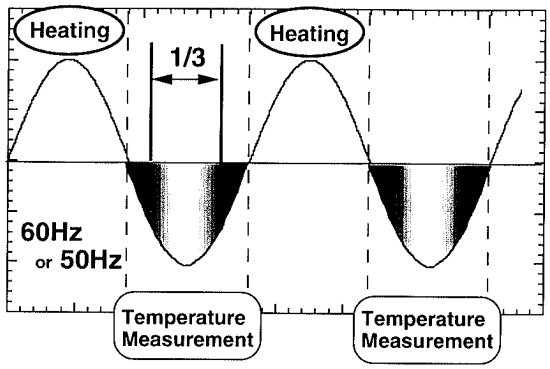

Fig. 1. Principle of hot thermocouple controller.

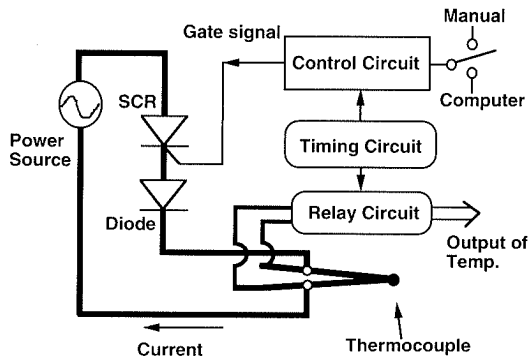

Fig. 2. Circuit diagram of the hot thermocouple controller.

(DHTT).

2. Experimental

2.1. Principle of Hot Thermocouple Driver

The hot thermocouple driver is a unique system that enables simultaneous measurement of temperature while a thermocouple is heated. In this method, the slag sample can be melted directly on the tip of the thermocouple or between two similarly configured thermocouples. **Figure 1** illustrates the principle of the hot-thermocouple controller. The electric current (60 Hz) is rectified into a half-wave by a silicon controlled rectifier (SCR), so that the heating cycle occurs for a maximum length of 1/120 sec followed by a similar period with no current input where the temperature of the thermocouple is measured using a relay circuit.

Figure 2 shows a circuit schematic of the hot thermocouple controller. The main circuit is the power supply circuit having a SCR and a diode. To control the SCR, the gate signal is supplied from the power control circuit (or temperature control circuit) which is operated by means of a computer or a potentiometer. Since the temperature will change with the length of thermocouple wire and the amount of sample, the temperature is not always constant when the same D.C. voltage is supplied to the control circuit. The output of electromotive force from thermocouple is connected to the relay circuit which is turned on only during one third of the no heating period to reduce sampling noise. All errors of temperature measurement occurring from a contact potential difference between the electrode and relay circuit were corrected by a calibration with pure CaF_2.

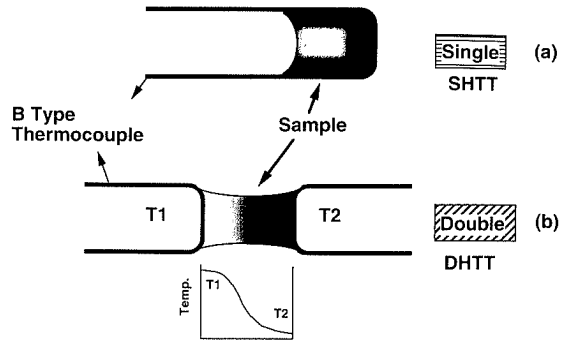

Fig. 3. Illustration of (b) double hot thermocouple technique (DHTT) and (a) single hot thermocouple technique (SHTT).

2.2. Single Hot Thermocouple Technique (SHTT) and Double Hot Thermocouple Technique (DHTT)

There are two modes of operation of the hot thermocouple technique. **Figure 3** shows the difference between single hot thermocouple and double hot thermocouple techniques. The first mode of operation is the single hot thermocouple technique (SHTT), which is the original development of the apparatus.[20-24] The SHTT is appropriate for samples of a high fluidity (or low viscosity) liquid such as calcium fluoride (CaF_2) and some mold slags.

The second mode of operation is the double hot thermocouple technique (DHTT), which was developed by the authors for mold slag crystallization studies. The DHTT has the advantage that a desired temperature gradient can be developed between the two thermocouples. Therefore, the temperature of the melt can be set and solidification initiated by controlling either the temperature or the temperature difference between the two thermocouples. In this method, it is possible to generate the various thermal gradient conditions which may be experienced in the mold of a steel continuous caster. For example, the slag sample can be completely melted and held isothermally on the thermocouples at temperatures which would be experienced in the mold of a continuous caster when the slag is in contact with the liquid steel (1 450–1 550°C) . One thermocouple can be then programmed with a desired cooling rate or rapidly decreased to a desired temperature to set a desired thermal gradient.

Most mold slags are based upon the lime-silica system with additions of other oxides and fluorides to extend the liquid phase field. Fortunately, the majority of the oxides used in mold slag formulations are transparent or translucent when liquid, while the crystals which precipitate tend to be opaque. Thus the crystallization phenomena can be clearly recorded using commercial video equipment and the onset of crystallization, the growth rate of the solidification front and its position can then be measured as a function of the cooling rate. Thus using the SHTT and the DHTT, solidification phenomena can be observed directly and the beginning of crystallization, the number of crystals, the morphology of the crystal and a kinetic analysis of the crystal growth rate can be performed either isothermally or under

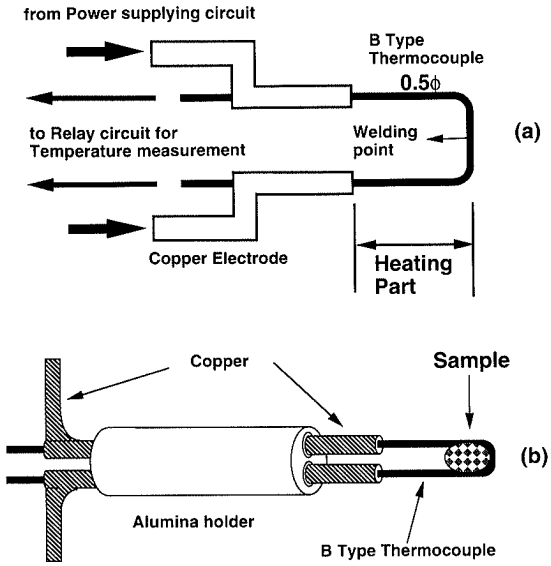

Fig. 4. Schematic of (a) electrode conjunction and (b) electrode assembly for hot thermocouple technique.

various thermal gradients.

There are limitations to the cooling rate that can be achieved using the SHTT and the DHTT and the maximum cooling rates which have been achieved are in excess of 150°C per second which is significantly higher than the critical cooling rate for glass formation measured for a number of similar oxide systems[24,28,29] and should allow TTT and CCT diagrams to be constructed for mold slags. Actual cooling rates between the steel shell and the mold of a continuous caster have been estimated by Ho and Thomas[30] to range from less than 1°C per second to 20°C per second depending upon position in the mold.

2.3. Experimental Apparatus

Figures 4(a) and **4(b)** show schematics of the electrode assembly and electrode used to hold a hot thermocouple. The one of most important technique is to weld the thermocouple without a bead and to make it same diameter. The wider or smaller diameter in hot thermocouple would result in a nonuniform heat generation. The thermocouple is heated from the tip of the thermocouple to the end of the copper electrode which is supplying the electric power. The maximum achievable temperature varies with the length of the thermocouple wire connected between the electrodes. The achievable cooling rate is a function of the length of the thermocouple wire and the heat transfer mechanism that controls heat loss from the sample. Tight contact between the thermocouple and copper electrode is important for noiseless measurement.

Figure 5 shows a schematic of the observed natural convection patterns of the gas flow around the sample. Kashiwaya *et al.* has investigated the effect of microgravity on the solidification of superconducting oxide[6] and has shown that the sample temperature increased under microgravity when natural convection was minimized, even though the power to the hot thermocouple was constant. Natural convection must be stabilized in this technique to obtain stable temperatures

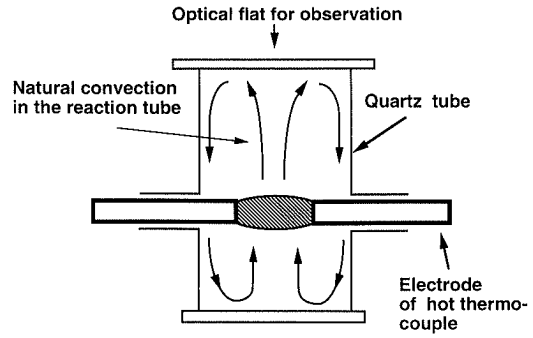

Fig. 5. Schematic of convection patterns in the reaction tube.

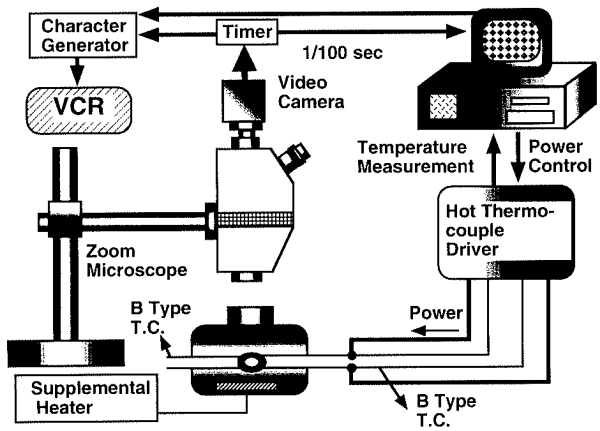

Fig. 6. Schematic of experimental apparatus. (VCR: video cassette recorder)

in the DHTT and SHTT. In the case of a large reaction tube, convection is unstable and it is difficult to reach an equilibrium temperature. Thus to establish a stable temperature for the hot thermocouple technique (HTT), the apparatus must have a small volume and a constant heat loss from the reaction tube to its surroundings. A supplemental heater was thus employed to minimize the heat loss from the surface of the sample to the ambient gas. Several types of supplemental heaters made out of platinum wire were adopted and located under the sample or adjacent to the sample.

Figure 6 shows the setup of the experimental apparatus which included the double hot thermocouple, the observation system and computer data acquisition system. The data acquisition system makes it possible to measure and control the sample temperature continuously and has a two channel D/A (digital–analog: 0–5 DC volt) interface that can control the hot thermocouples independently. The sample is 3 mm in diameter; therefore, an optical microscope connected to a CCD camera was used to allow observation of the sample. As the video signal does not have the information of experimental time and temperature, a superimposer of time and characters which exhibits the experimental conditions was connected to the video system. The computer has an image capturing system which allows a more detailed analysis of the crystallization phenomena, allows real time digital storage of the signal and allows "post mortem" analysis of the rate of crystal growth.

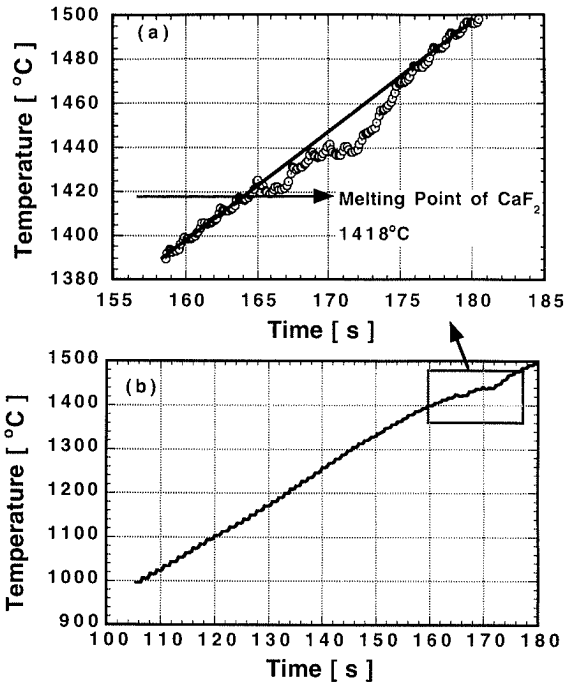

Fig. 7. Temperature profile of hot thermocouple, when reagent CaF_2 was melted.

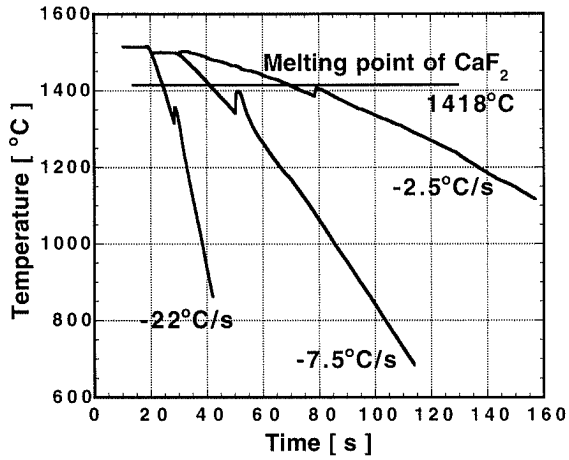

Fig. 8. Recalescene behavior of CaF_2 at different cooling rates using SHTT.

2.4. Calibration of Hot Thermocouple

In order to calibrate the temperature which is measured by the DHTT and the SHTT, experiments were carried out with calcium fluoride (CaF_2), a material having known thermophysical properties. **Figure 7** shows the results of the experiments using the SHTT with CaF_2 with a programmed linear heating rate. As mentioned above, the SHTT was used owing to the sample's low viscosity. Figure 7(b) shows the variation of temperature with time from 1 000°C to the melting point of CaF_2. Figure 7(a) expands the temperature range near the melting point. The average heating rate was 7.4°C/s (444°C/min). The temperature profile was linear over the first 10 to 20 sec. A deviation in the heating curve occurred at 1 423°C which was in good agreement with the melting point of CaF_2, 1 418°C.

The SHTT was then operated in a similar fashion to a DTA and temperature-time curves for different cooling rates are shown in **Fig. 8** for the solidification of CaF_2. It was found that general relationships between the cooling rate and the degree of undercooling and recalescence could be obtained. When a slower cooling rate or heating rate was selected, more exact melting points were obtained. The beginning of crystallization could be determined not only by direct observation but also by temperature measurement in this experiment. Accordingly, the SHTT could also be used to study opaque pure liquids. Thermal effects are more evident in a pure material that has a defined melting point. In a mold slag, crystal nucleation and growth may occur over a wide range of temperature, making a deviation from the cooling curve indistinct. Thus in complex systems it is necessary to work with transparent systems where the crystal growth can be observed.

3. Results and Discussions

In situ observations of the solidification behavior of slags have been performed using both the DHTT and the SHTT. In this study, the results of *in situ* observation of mold slag crystallization will be shown and the potential of the DHTT and the SHTT will be discussed and applied to the problem of mold slag crystallization.

Figure 9 shows the melting behavior of a simulated mold slag during heating. The chemical composition of the slag was 5 mass% Na_2O, 6.7 mass% Al_2O_3, 44 mass% CaO and 44 mass% SiO_2. Bubbles were formed inside the sample during melting. In this experiment, reagent grade sodium oxide was mixed into a mother slag which was melted in a graphite crucible and crushed into a powder (under 100 μm) to minimize sodium oxide loss by vaporization during preparation. In the melting of industrial mold slags, bubble evolution during melting was also observed. Thus the technique allows melting phenomena to be studied. In addition during heating the transparency of the melt went through a number of variations and the technique may be useful for the determination of the optical properties of slags.

Figure 10 shows the melt after it had become clear and transparent at 1 550°C. The sample forms a lens and an image of the coils of the supplemental heater below the sample can be observed clearly in the figure. However, this image of the hot heating wires below the sample disturbed the observation of small crystals during an experiment and the supplemental heater was subsequently modified and platinum wire was folded into a zigzag pattern and placed around the apparatus to concentrate the heat around the sample. This rearrangement allowed a clear image of the lens.

Figure 11 shows the temperature profiles of the DHTT when experiments were carried out to simulate the thermal conditions which may be found in the mold of a continuous caster. The right hand side thermocouple (Ch-1) was cooled at a constant rate and the left hand side thermocouple (Ch-2) was maintained with a constant power input to attempt to hold the temperature constant. In these experiments, the cooling rate was varied from 15 to 80°C/s to simulate the maximum range of cooling

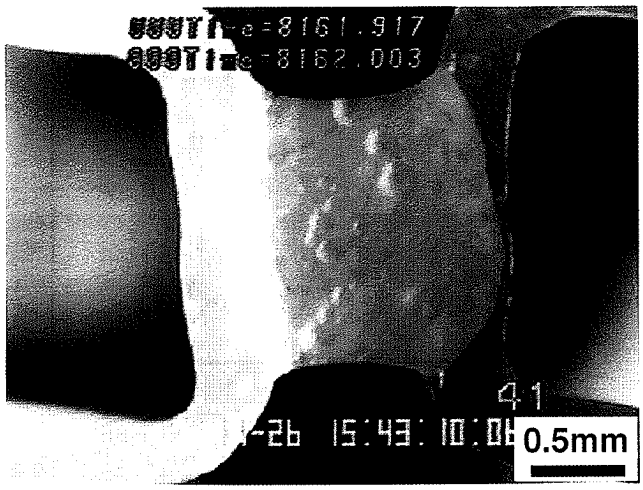

Fig. 9. Result of *in situ* observation by DHTT. Melting behavior of a simulated mold slag. (5% Na_2O, 6.8% Al_2O_3, C/S=1)

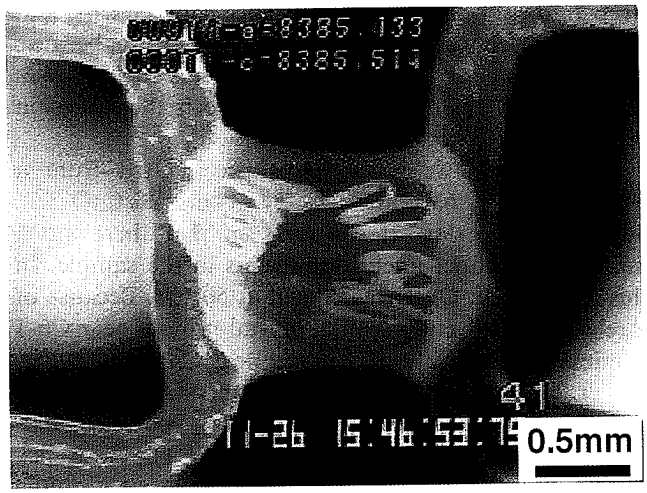

Fig. 10. Result of *in situ* observation by DHTT of a simulated mold slag at 1 550°C. (5% Na_2O, 6.8% Al_2O_3, C/S=1)

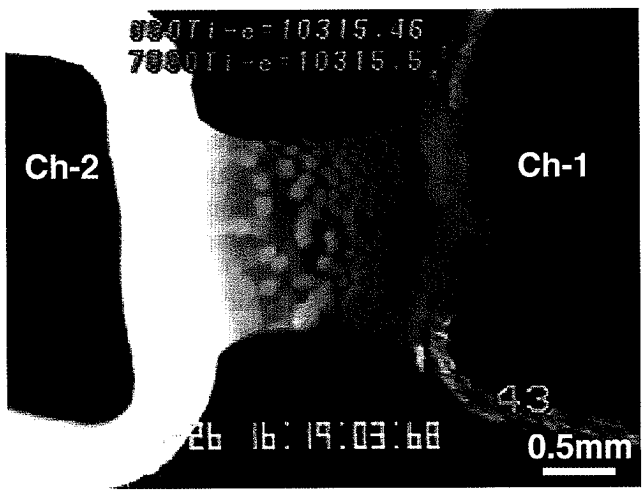

Fig. 13. Crystallization behavior of a simulated mold slag when Ch-1 was cooled with 50°C/s. (5% Na_2O, 6.8% Al_2O_3, C/S=1)

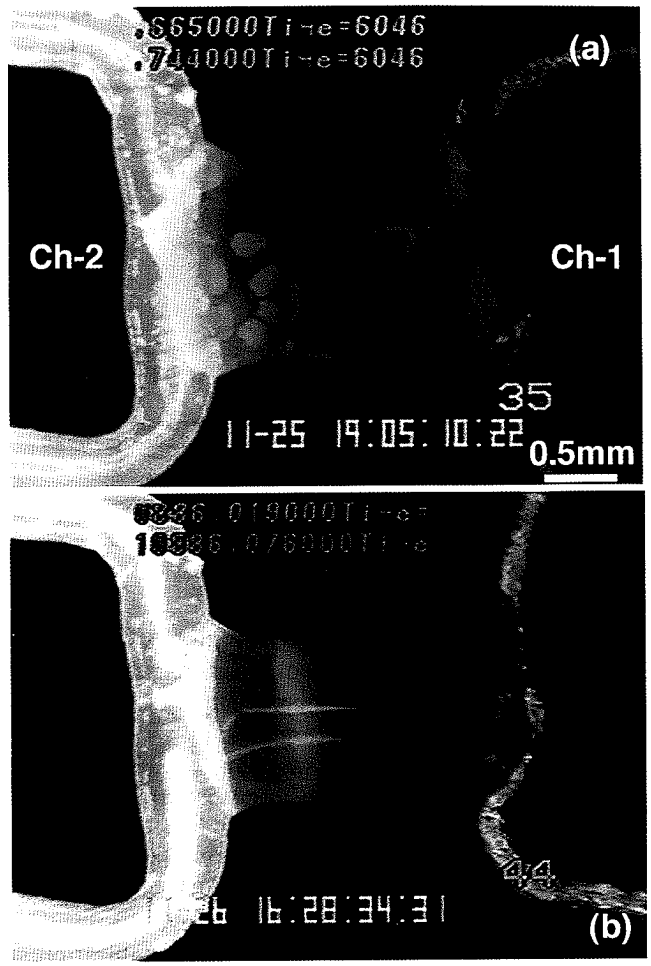

Fig. 14. Crystallization behavior of simulated mold slags.
(a) 50°C/s (3.8% Na_2O, 6.8% Al_2O_3, C/S=1)
(b) 80°C/s (5% Na_2O, 6.7% Al_2O_3, C/S=1)

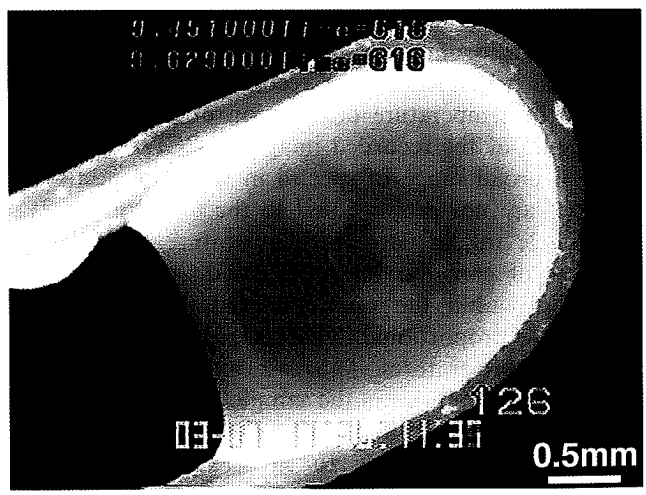

Fig. 15. Crystallization behavior of industrial mold slag by SHTT in isothermal experiment for TTT diagram (1 215°C).

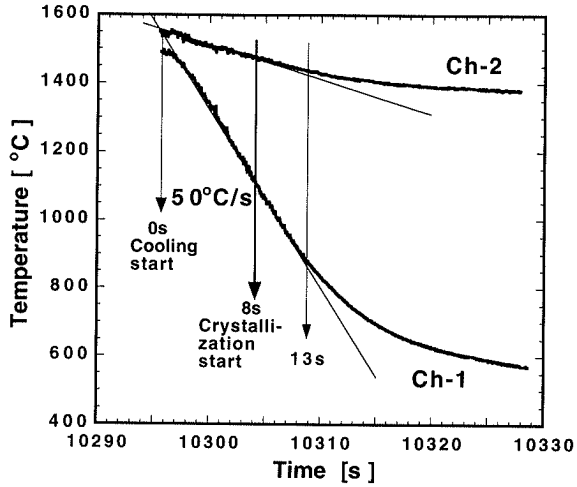

Fig. 11. Temperature profiles of double hot thermocouple during a non-isothermal experiment simulating the continuous caster.

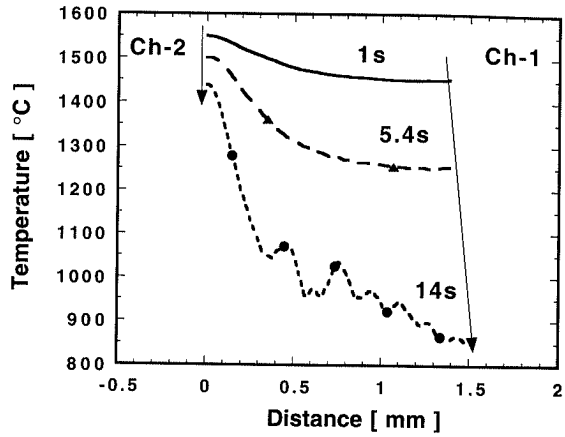

Fig. 12. Variation of temperature distributions of the sample estimated from the image brightness.

rates that might be found in a continuous caster mold slag. In Fig. 11, Ch-1 was cooled with a rate of 50°C/s and the details of the results under other conditions will be published in the near future.[31]

The cooling rate of Ch-1 was constant for 8 sec until the temperature reached 880°C. The temperature of Ch-2 decreased from 1 550 to 1 450°C within 13 sec from the start of cooling, even though the power input was constant. Small crystals were observed after 8 sec in video image and the cooling rate of Ch-2 changed at this time, because of the exothermic nature of crystallization. If there was no heat evolution inside the sample and Ch-1 cooled with a constant rate, Ch-2 would have a constant cooling rate. In this case, the position of the deviation from a straight line occurred at the same time as the *in situ* observation of crystallization.

One of disadvantages of this method arises due to the difficulty in the determination of the temperature profile in the sample. It is possible, however, to estimate the temperature profile of sample between Ch-1 and Ch-2 from the brightness of the recorded image. **Figure 12** shows the temperature distribution obtained from the brightness of the recorded image. A CCD camera can sense a broad range of spectra in which respective intensities are not proportional to the temperature. It is impossible to compare the temperature from the intensities of emission between two different materials, however, within the same material, the intensity of emission is proportional to the temperature over a short range of temperatures. Thus we can estimate the temperature distributions in the sample from the brightness of the image as the temperatures of the two points in each image are known. In Fig. 12, the intensity of brightness of the sample in the vicinity of the Ch-1 and Ch-2 thermocouple were assumed to be equal to the temperature recorded by the thermocouples. Then using the coefficient derived from the measurement, the temperature distribution across the sample was estimated. The profiles were smooth (after 1 and 5.4 s in Fig. 12) until crystals precipitated, and became irregular after the crystal precipitated, probably due to the latent heat of crystallization and a change in the emissivity due to the presence of the crystal fraction. The temperature distributions within 0.8 mm from Ch-1 (0.7 mm from Ch-2) in Fig. 12 (1 and 5.4 s) were almost flat with a steep gradient near Ch-2. The distance between Ch-1 and Ch-2 increased with the decreasing temperature, because of the contraction of thermocouple. Thus the arrow in Fig. 12 at Ch-1 is not vertical and reflects the extension of the sample during the experiment.

Figure 13 shows the crystals precipitated from a 5 mass% Na_2O, 6.8 mass% Al_2O_3, 44 mass% CaO and 44 mass% SiO_2 slag. It can be seen that there are a number of distinct nucleation events in the sample. In this experiment, Ch-1 was cooled at 50°C/s. Because of a relatively high cooling rate, crystal growth near Ch-1 is minimized and crystals coarsen near Ch-2, due to the higher temperature and enhanced crystal growth by diffusion. This result is typical of the type of crystallization that was observed in these slags. The frequency of precipitated crystals could be varied by varying cooling rate. This crystallization phenomenon is typical of the type that one would expect due to nucleation and growth from an undercooled melt. In addition the morphology of the crystals varied from dendritic at high cooling rates to blocky faceted crystals at lower cooling rates.

Figure 14 shows the effect of the cooling rate on the morphology of crystal in simulated mold slags at 50°C/s (Fig. 14(a): 3.8 mass% Na_2O, 6.8 mass% Al_2O_3, 45 mass% CaO and 45 mass% SiO_2) and 80°C/s (Fig. 14(b): 5 mass% Na_2O, 6.7 mass% Al_2O_3, 44.3 mass% CaO and 44.3 mass% SiO_2)). Figure 14(a) is the image after 17 s from the beginning of crystallization and Fig. 14(b) is an image after 16 s from the beginning of crystallization. If one compares Fig. 13 to Fig. 14 (a), one can see that when the amount of sodium oxide is decreased, the frequency of crystallization is decreased and a glassy phase is stabilized. Thus in this system the crystallization frequency is very sensitive to the sodium oxide content in the slag. At higher cooling rates (Fig. 14 (b)) glass formation can be clearly observed and the crystals are not clearly visible but the heat signature denoting the onset of crystallization can be clearly seen. In Fig. 14(b), a fine crystal layer precipitated in the sample in the area where the heat signature was noted during visual ob-

servation. SEM analysis on a quenched specimen confirmed the presence of small dendritic crystals in the glass in this region.

Figure 15 shows the result of an isothermal experiment to determine the crystallization behavior of an industrial mold slag used in the continuous casting of austenitic stainless steels. The chemical composition of the slag was 37.8 mass% SiO_2, 33.3 mass% CaO, 7.9 mass% Al_2O_3, 8.2 mass% Na_2O and 8.4 mass% F. In this case, the powder was decarburized by the manufacturer in order to facilitate the experiment. The viscosity of industrial mold slag was quite low and it was difficult to hold the sample between two thermocouples in the DHTT and the SHTT was used to allow crystallization to be measured during an isothermal hold. The sample was melted at 1 500°C to eliminate the bubbles, held for 4–5 min to allow homogenization, cooled to a given temperature with a high cooling rate (≈80°C/s) and then held for 30 to 60 min until crystallization was complete. In all cases bubble formation was observed during the melting process. Crystallization initiated within 10 to 400 sec of isothermal holding (depending on the temperature) and the crystals grew for up to 45 min after the initiation of crystallization.

It was found that the shape of the crystals and the mode of crystal growth were quite different between the isothermal experiment and the nonisothermal experiment which simulated the cooling conditions of the continuous caster. Thus both isothermal and nonisothermal experimentation will be important in the understanding of the behavior of a mold slag in an actual system.

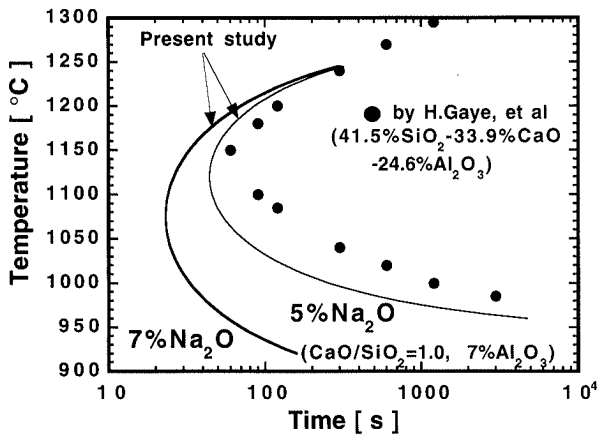

Fig. 16. Effects of Na_2O on TTT curve obtained by present study and Gaye *et al.*

These techniques appear to be quite versatile and have already shown that it is possible to observe crystal growth under defined thermal conditions, to modify crystal frequency and morphology with variations in the cooling rate and to measure thermal effects relating to crystallization simultaneously with observation of the phenomena. The technique allows the possibility of a fast and accurate determination of both TTT and CCT curves in transparent slag systems.

Figure 16 shows a TTT diagram for lime–alumina–silica slags containing sodium oxide. The beginning of crystallization was determined by the direct observation using DHTT or SHTT. To develop the TTT diagram, X-ray diffractions were carried out to determine the crystalline phase after quenching the sample to room temperature. The TTT curves for these simulated mold slags containing 5 % Na_2O and 7 % Na_2O (the composition of mother slag is 7 mass% Al_2O_3, $CaO/SiO_2 = 1.0$), were obtained by the DHTT and are compared with the data from Gaye *et al.*[32] on a lime silica alumina slag where the TTT was determined by an isothermal hold and quench technique. The data for TTT curves on 5 mass% Na_2O and 7 mass% Na_2O had relatively large scattering, then the empirical formulae were used to expressed the data. The details of the data and formulae will be published also. Although the composition of slag in $CaO–SiO_2–Al_2O_3$ system was different from the present study, the results indicate that additions of sodium oxide cause a major alteration to the TTT curve. The temperature of the nose decreased with the content of sodium oxide and the incubation time of crystallization decreased with the sodium oxide content. Thus the critical cooling rate to stabilize the glassy phase increased with increasing sodium oxide content.

Figures 17(a) and **17(b)** show the crystal morphology captured during crystal growth in the simulated slag melt containing 7 % Na_2O at 1 300 and 1 140°C, respectively. At the higher temperature (Fig. 17(a)), the crystal grew macroscopically as an equiaxed dendrite. Figure 17(b) shows a macroscopic cubic crystal, however, dendritic growth was observed at the solidification front in each face of the cube. Thus the morphology of crystal drastically changed with decreasing temperature. The DHTT and the SHTT provide new information about

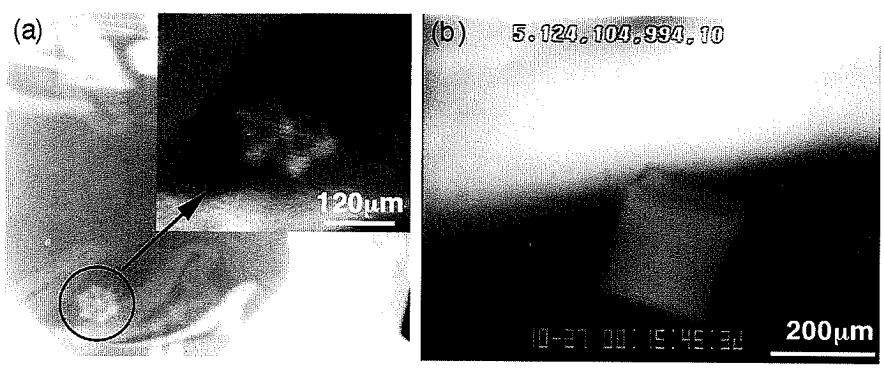

Fig. 17. Crystal morphology precipitated from undercooled melt.
(a) dendritic crystal at 1 300°C (b) cubic crystal at 1 140°C

crystal growth of mold slag, and it will be possible to quantitatively clarify the crystallization phenomena of mold slag using these techniques.

4. Summary

The double and single hot thermocouple techniques (DHTT and SHTT) were developed for the *in situ* observation of mold slag crystallization. Important information on the crystallization behavior of a mold slag can be obtained with these techniques under both non-isothermal and isothermal conditions and examples of variation in crystal frequency and growth morphology as a function of cooling rate can be measured. Using these techniques, it will be possible to obtain a more detailed understanding of silicate slag crystallization phenomena.

REFERENCES

1) M. Wolf: ISS Process Technology Conf., 13, (1995), 99.
2) M. Emi: ISS Steelmaking Proc., (1991), 623.
3) P. Riboud and M. Larrecq: ISS Steelmaking Proc., (1979), 78.
4) H. Kyoden, T. Doihara and O. Nomura: ISS Steelmaking Proc., (1986), 153.
5) K. Mills, M. Susa and V. Ludlow: ISS Process Technology Conf., 13, (1995), 157.
6) A. Yamauchi, K. Sorimachi, T. Sakuraya and T. Fuji: *ISIJ Int.*, **33** (1993), 140.
7) M. Jenkins: ISS Steelmaking Proc., (1995), 315.
8) H. Shibata, J. Cho, T. Emi and M. Suzuki: Molten Slags, Fluxes and Salts '97 Conf., (1997), 771.
9) L. Hering, H. Heller and H. Fenzke: *Stahl Eisen*, **112** (1992), 61.
10) H. Nakato, T. Sakuraya, T. Nozaki, T. Emi and H. Nishikawa: ISS Steelmaking Proc., (1986), 137.
11) H. Lindenberg and J. Loh: ISS Steelmaking Proc., (1986), 161.
12) K. Sorimachi, M. Kuga, H. Nishikawa, K. Marumoto and H. Nakato: *Trans. Iron Steel Inst. Jpn.*, **21** (1982), B-435.
13) K. Sorimachi, M. Kuga, M. Saigusa and T. Sakuraya: *Fachber. Hütttenprax. Metallweiterverarb.*, **20** (1982), 244.
14) S. Chang, I. Lee, M. Kim, S. Yang, J. Choi and J. Park: Conf. on Continuous Casting of Steel in Developing Countries, China, (1993), 832.
15) H. Gilles, M. Byrne, T. Ruso and G. DeMasi: ISS Process Technology Conf. Proc., (1990), 123.
16) H. Sakai, T. Kawashima, T. Shiomi, K. Watanabe and T. Iida: Molten Slags, Fluxes and Salts '97 Conf., (1997), 787.
17) K. Watanabe, M. Suzuki, K. Murakami, H. Kondo, A. Miyamoto and T. Shiomi: *Tetsu-to-Hagané*, **83** (1997), 31.
18) M. Bhamra, M. Charlesworth, S. Wong, D. Sawyers-Villers and A. Cramb: ISS Electric Furnace Conf., (1996), 551.
19) R. Bommaraju: ISS Steelmaking Proc., (1991), 131.
20) F. Ordway: *J. Res. Natl. Bur. Stand.*, **48** (1952), 512.
21) J. H. Welch: *J. Sci. Instrm.*, **31** (1954), 458.
22) T. Yanagase, F. Noguchi and Y. Ueda: Proc. of Int. Conf. Sci. and Techn. Iron and Steel, (1971), 516.
23) Y. Ohta, K. Morinaga and T. Yanagase: *Bull. Jpn. Inst. Met.*, **19** (1980), 139.
24) E. Asayama, H. Takebe and K. Morinaga: *ISIJ Int.*, **33** (1993), 233.
25) Y. Kashiwaya, D. Jukawa and K. Ishii: JASMAC-8, (1992).
26) Y. Murayama, Y. Kashiwaya and K. Ishii: *CAMP-ISIJ*, **7** (1994), 891.
27) T. Kuranaga, Y. Kashiwaya and K. Ishii: Int. Symp. on Adv. Mat. and Tech. for 21st Cent. JIM '95 Fall Meeting, Honolulu, (1995).
28) H. Scholze: Glass, Springer-Verlag, Berlin, (1991).
29) D. R. Uhlman: *J. Am. Ceram. Soc.*, **66** (1983), 95.
30) B. Ho: Characterization of Interfacial Heat Transfer in the Continuous Slab Casting Process, Masters Thesis, University of Illinois–Champagne, (1992).
31) Y. Kashiwaya, C. E. Cicutti and A. W. Cramb: *Tetsu-to-Hagané*, to be submitted.
32) H. Gaye, C. Gatellier and P.V. Riboud: Turkdogan Symp. Proc., (1994), 113.